STATIONARY SUPERSONIC CONDUCTING GAS FLOW IN A CHANNEL WITH NONCONDUCTING WALLS UNDER WEAK MAGNETOHYDRODYNAMIC INTERACTION

E. K. Kholshchevnikova

A solution of the problem of flow in a channel with nonconducting walls for a small magnetohydrodynamic interaction parameter N is obtained by numerical methods. In the 0-10 range of variation of the Hall and magnetic Reynolds number parameters the distributions of the electrical parameters and the average (over the cross section) and local gasdynamic flow parameters are computed for two different geometries of the applied magnetic field. It is shown that an increase in the Hall and magnetic Reynolds number parameters is accompanied by a diminution in the Joule dissipation and the perturbation of the average (over the cross section) gasdynamic flow characteristics. It is disclosed that the distribution of the gasdynamic parameters over the channel cross section is extremely nonmonotonic in the end current zones.

When studying different magnetohydrodynamic apparatus, it is very important to clarify the influence of the zone of magnetic-field inhomogeneity on the flow characteristics. The system of equations describing the gas flow in such zones includes the gasdynamics equation (with electromagnetic forces and Joule dissipation inserted in addition) and the electrodynamics equations for the electrical currents, the potential, and the magnetic field. For a small parameter N, the electrodynamics equations are solved independently of the gasdynamics equations, and the distributions of the electrodynamic forces and Joule-heat liberation found with their use are then utilized in the gasdynamics equations to determine the perturbed gas flow.

An extensive bibliography [1-7] is devoted, at present, to the analysis of the electrical field in channels by means of given distributions of the gasdynamics parameters. The basic factors affecting the electrical field are the geometry of the applied magnetic field, the Hall parameter β, and the magnetic Reynolds number R_m. The influence of each of these factors is examined separately in the papers listed. The combined influence of the paramters β and R_m is considered in [6, 7], but for the simplest magnetic-field geometry. The solutions presented in the papers have been obtained by analytical methods.

The method of small parameters (see [8], for instance) is also utilized in magnetic hydrodynamics. Comparatively few papers [9-11] are devoted to the analyses of supersonic gas flows in channels with end magnetic-field zones. The computations presented were hence limited to cases of special magnetic-field geometry and $\beta = 0$, $R_m = 0$.

The influence of the Hall parameter and the magnetic Reynolds number on the electrical and gasdynamic characteristics of a conducting gas flow is studied below in zones of magnetic-field inhomogeneity for a small interaction parameter N.

1. Let us consider the motion of a perfect gas with constant specific heats and constant conductivity σ in a plane channel $|x| < \infty$, $0 \leq y \leq h$ with nonconducting walls (Fig. 1) in the presence of an external inhomogeneous magnetic field, which can be represented after averaging over the transverse coordinate z as

$$B_e = (0, 0, B_e(x))$$

Moscow. Translated from Zhurnal Prikladnoi Mekhaniki i Tekhnicheskoi Fiziki, No. 4, pp. 20-29, July-August, 1970. Original article submitted April 3, 1970.

The system of magnetohydrodynamic equations includes the continuity, motion, energy, Ohm's law, and Maxwell equations. For $N \ll 1$ the equations can be linearized with respect to this parameter [8].

In a first approximation the solution of the system of equations is sought in the form

$$\mathbf{v} = \mathbf{v}_0 + N\mathbf{v}_1, \quad p = p_0 + Np_1, \quad \rho = \rho_0 + N\rho_1$$
$$\mathbf{B} = \mathbf{B}_0 + N\mathbf{B}_1, \quad \varphi = \varphi_0 + N\varphi_1, \quad \mathbf{j} = \mathbf{j}_0 + N\mathbf{j}_1$$

Here $\mathbf{v}$ is the velocity, p is the pressure, ρ is the gas density, $\mathbf{B}$ is the magnetic-field induction, φ is the electrical potential, $\mathbf{j}$ is the current-density vector; the subscript 0 denotes the flow parameters undisturbed by the magnetic field and the electrical quantities computed by means of the undisturbed gasdynamic parameters, while the subscript 1 denotes the perturbations in the gasdynamic and electrical quantities.

It has been shown in [8] that the system of gasdynamics equations for a flow undisturbed by the magnetic field in a plane channel will be satisfied by the distributions

$$\mathbf{v}_0 = (u_0(y), 0, 0), \quad \rho_0 = \rho_0(y), \quad p_0 = \text{const} \tag{1.1}$$

The Maxwell and Ohm's law equations are in the case under consideration

$$\mathbf{j}_0 = -\nabla\varphi_0 + \mathbf{v}_0 \times \mathbf{b}_0 - \beta_0 \mathbf{j}_0 \times \mathbf{b}_0 \tag{1.2}$$
$$\operatorname{rot} \mathbf{b}_0 = R_m \mathbf{j}_0, \quad \operatorname{div} \mathbf{j}_0 = 0, \quad \operatorname{div} \mathbf{b}_0 = 0$$

Following [8], let us write the equations for the perturbations of the gasdynamic parameters for $\rho_0 = u_0 = 1$:

$$\frac{\partial u_1}{\partial x} + \frac{\partial p_1}{\partial x} = f_x, \quad \frac{\partial v_1}{\partial x} + \frac{\partial p_1}{\partial y} = f_y \tag{1.3}$$
$$\frac{\partial \rho_1}{\partial x} + \frac{\partial u_1}{\partial x} + \frac{\partial v_1}{\partial y} = 0, \quad \frac{\partial p_1}{\partial x} - a_0^2 \frac{\partial \rho_1}{\partial x} = q$$
$$f_x = j_{y0} b_0, \quad f_y = -j_{x0} b_0, \quad q = (\gamma - 1)(j_{x0}^2 + j_{y0}^2), \quad a_0 = 1/M_0$$

Here a_0 and M_0 are the speed of sound and the Mach number of the unperturbed flow, γ is the ratio between the specific heats, u_1 and v_1 are components of the perturbed velocity vector; the magnitudes of the electromagnetic forces $f = (f_x, f_y)$ and the Joule dissipation q are assumed known from the solution of the system (1.2).

The systems (1.2) and (1.3) are written in dimensionless variables which are introduced by means of the following formulas:

$$\mathbf{v}^\circ = U\mathbf{v}, \quad \mathbf{B} = B^*\mathbf{b}, \quad x^\circ = xh, \quad y^\circ = yh, \quad \rho^\circ = \rho^*\rho, \quad p^\circ = \rho^* U^2 p$$
$$\mathbf{j}^\circ = \frac{\sigma^* U B^*}{c}\mathbf{j}, \quad \varphi^\circ = \frac{UB^*h}{c}\varphi, \quad \beta = \frac{e\tau B^*}{mc}, \quad R_m = \frac{4\pi\sigma^* U h}{c^2} \tag{1.4}$$

Here U is the average velocity (over the cross section) at the entrance to the channel, h is the channel height, B^*, ρ^*, σ^* are the characteristic magnetic induction, density, and electrical conductivity, e and m are the electron charge and mass, τ is the time between electron collisions with an ion, and c is the speed of sound in a vacuum; the degree symbol denotes dimensional quantities.

The interaction parameter N by means of which the linearization is carried out is defined as follows:

$$N = \frac{\sigma^* B^{*2} h}{c^2 \rho^* U}$$

Let us utilize the condition that the normal current j_y does not flow through the upper and lower walls of the channel and the condition of no longitudinal current j_x at $\pm\infty$ as the boundary conditions for the solution of the system (1.2).

Let us consider that there is no electromagnetic field at the channel entrance (for $x \to -\infty$), and therefore, the perturbations of all the gasdynamic quantities are zero. Therefore, the boundary conditions for the solution of the system (1.3) are

$$u_1 = v_1 = p_1 = \rho_1 = 0 \text{ at } x \to -\infty$$

Moreover, from the condition that the fluid does not flow through the upper and lower channel walls we will have, for the transverse velocity component,

$$v_1 = 0 \quad \text{at} \quad y = 0, \quad y = 1$$

Let us note that from the system (1.3) it is easy to find the gasdynamic parameters, averaged over the channel cross section. Indeed, let us integrate the first, third, and fourth equations of the system (1.3) over the channel cross section. We then obtain the following equations for the averaged quantities:

$$\frac{d\langle u_1\rangle}{dx} + \frac{d\langle p_1\rangle}{dx} = \langle f_x\rangle, \qquad \frac{d\langle \rho_1\rangle}{dx} + \frac{d\langle u_1\rangle}{dx} = 0 \tag{1.5}$$

$$\frac{d\langle p_1\rangle}{dx} - \frac{1}{M_0^2}\frac{d\langle \rho_1\rangle}{dx} = \langle q\rangle, \quad \langle \varkappa\rangle = \int_0^1 \varkappa dy, \quad M_0 = \text{const}$$

2. Let us turn to the electrical part of the problem. For convenience, let us omit the subscript 0 from the electrical quantities in the system (1.2). Let us represent the magnetic field in the form of the sum

$$\mathbf{b} = \mathbf{b}_e + \mathbf{b}_i \tag{2.1}$$

Here $\mathbf{b}_e$ is the applied field, and $\mathbf{b}_i$ is the induced field caused by currents flowing in the gas.

The real external field $\mathbf{b}_e$ always satisfies the equation rot $\mathbf{b}_e = 0$. We hence obtain from (1.2)

$$\operatorname{rot} \mathbf{b}_i = R_m \mathbf{j} \tag{2.2}$$

Let us average the Ohm's law (1.2) and Eq. (2.2) with respect to the coordinate z. Neglecting the correlation terms and considering the unperturbed velocity vector to have just the longitudinal component $u_0(y)$ [see (1.1)] and the magnetic field projections b_x and b_y on the coordinate axes to be zero on the walls z = const, we obtain from (1.2) and (2.2)

$$j_x = -\frac{\partial \varphi}{\partial x} - \beta j_y b, \qquad j_y = -\frac{\partial \varphi}{\partial y} - u_0 b + \beta j_x b$$

$$j_x = \frac{1}{R_m}\frac{\partial b_i}{\partial y}, \qquad j_y = -\frac{1}{R_m}\frac{\partial b_i}{\partial x}, \qquad \mathbf{b} = (0, 0, b(x)), \quad b = b_e + b_i \tag{2.3}$$

Here j_x, j_y, φ, b, b_e, b_i are quantities averaged with respect to the coordinate z.

Differentiating j_x with respect to y, j_y with respect to x and subtracting the second expression from the first, we will have after manipulation

$$\frac{\partial^2 b_i^*}{\partial x^2} + \frac{\partial^2 b_i^*}{\partial y^2} - R_m u_0 \frac{\partial b_i^*}{\partial x} + \beta \frac{db_e}{dx}\frac{\partial b_i^*}{\partial y} = u_0 \frac{db_e}{dx} \tag{2.4}$$

$$b_i^* = \frac{b_i}{R_m}, \qquad j_x = \frac{\partial b_i^*}{\partial y}, \qquad j_y = -\frac{\partial b_i^*}{\partial x} \tag{2.5}$$

Let us consider the boundary conditions needed for the solution of (2.4). As has been mentioned above,

$$j_y = 0 \quad \text{at} \quad y = 0, \; y = 1; \qquad j_x = 0 \quad \text{at} \quad x = \pm\infty \tag{2.6}$$

Since the end currents are quite small, in practice, at distances on the order of several calibers (h) from the domains of an abrupt change in the magnetic field, then the left and right channel boundaries can be selected in place of $\pm\infty$ in such a way that they would be at a finite but sufficiently remote distance from the mentioned domains (Fig. 1). Hence, taking account of (2.5), we obtain the following boundary conditions to solve (2.4):

$$b_i^* = 0 \quad \text{at} \quad y = 0, \; y = 1; \qquad b_i^* = 0 \quad \text{at} \quad x = x_1, \; x = x_2 \tag{2.7}$$

It is seen from (2.4) that for a homogeneous applied field b_e, the term dependent on the Hall parameter β will not enter this equation. In this case the parameter β can influence the solution of the problem by means of the boundary conditions, for example, if there are portions of the channel walls occupied by electrodes. In cases when the parameter β does not enter the boundary conditions, the distributions of the electrical currents and the induced fields are independent of the effect of anisotropy of the conductivity; however, the distribution of the electrical potential is a function of the parameter β (see [7]), as follows from Ohm's law.

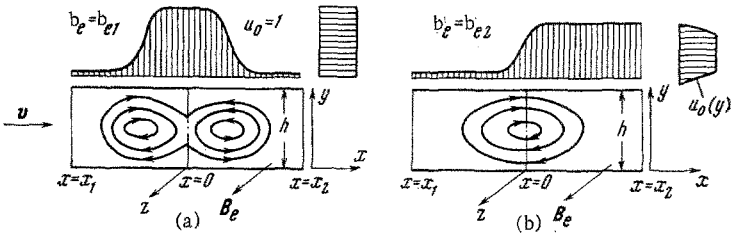

Fig. 1

Using the Ohm's law (2.3), Eq. (2.5), and the boundary conditions (2.6) and (2.7), some useful relations can be obtained.

Indeed, let us integrate (2.3) for j_x with respect to y between 0 and 1 and with respect to x between $-\infty$ and $+\infty$. Then taking into account that in a channel of unit width with nonconducting walls and constant velocity $v = u_0 = 1$, the dimensionless Joule dissipation is determined by

$$Q = -\int_{-\infty}^{+\infty}\int_{0}^{1} j_y b\,dx\,dy \tag{2.8}$$

and putting $\varphi(-\infty, y) = 0$, we arrive at the equality

$$\langle\varphi_+\rangle = \int_0^1 \varphi(+\infty, y)\,dy = \beta Q \tag{2.9}$$

If $b(+\infty) = 0$, then from the expression (2.3) for j_y it follows that the potential at $+\infty$ is independent of y. In this case we will have in place of (2.9)

$$\varphi(+\infty) = \beta Q \tag{2.10}$$

Therefore, the relations (2.9) and (2.10) connect the magnitude of the Joule dissipation with the longitudinal potential difference in the presence of anisotropy in the conductivity.

When the Hall parameter β is zero and the current picture is symmetrical relative to the channel axis, the following expression for the Joule dissipation can be obtained from (2.8):

$$Q = 2\int_{-\infty}^{+\infty} \frac{db_e}{dx} I_1(x)\,dx, \qquad I_1(x) = \int_{1/2}^{1} (y - 1/2)\, j_x(x, y)\,dy \tag{2.11}$$

Let us note that the magnitude of the end current flowing through a given channel cross section is defined by

$$I(x) = \int_{1/2}^{1} j_x(x, y)\,dy$$

This quantity is usually measured in experiments by a Rogowski coil. Computations showed that the ratio between the quantities I and I_1 is a slightly varying function and fluctuates between the limits 2.4-3.4. For the majority of cases $I/I_1 \approx 3$. Utilizing this relationship, I_1 can be found by means of the values of I found in experiments, and the approximate value of Joule dissipation is calculated by means of (2.11). Since the product of db_e/dx by I_1 enters in the integrand of the formula for Q, this product will introduce the main contribution to Q in the zones of abrupt changes in the magnetic field, where the derivative db_e/dx is large. The extent of such zones is usually small, and hence an approximate estimate of Joule dissipation by (2.11) is not difficult.

3. Equation (2.4) is an equation of elliptic type. One of the iteration methods, the method of successive displacements (Zeidel' method) with acceleration by the Lyusternik formula (see [12, 13]), was utilized to solve this equation. Writing (2.4) in finite differences corresponded to a five-point approximation of a second-order differential equation. The error in calculating the induced field b_i^* was hence a quantity on the order of the square of the mesh spacing $O(h^2)$.

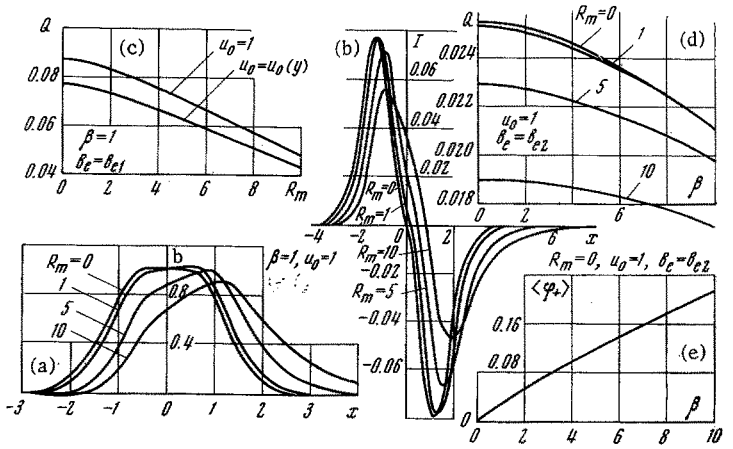

Fig. 2

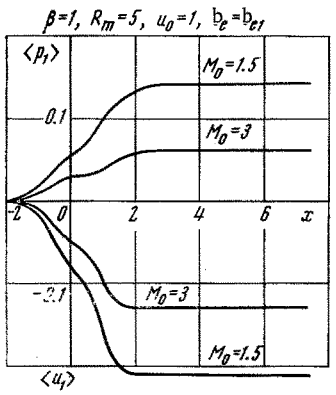

Fig. 3

The following values of the parameters were selected for the computation:

$$\beta = 0{,}1,\ 3,\ 5,\ 10;\ R_m = 0,\ 1,\ 5,\ 10;\ x_1 = -3.5$$
$$x_2 = 3.5,\ h = 0.1 \text{ at } R_m = 0; \quad x_2 = 4.5,\ h = 0.1 \text{ at } R_m = 1 \qquad (3.1)$$
$$x_2 = 7.5,\ h = 1/8 \text{ at } R_m = 5; \quad x_2 = 9.5,\ h = 1/8 \text{ at } R_m = 10$$

The right boundary of the channel x_2 was chosen in such a way as to take account of the stagger of the end currents in the longitudinal direction for large values of R_m (see [7]). The tendency of j_y to zero on approaching the right boundary was the criterion for the correctness of the selection of x_2. The values of the mesh spacing h were bounded by the operational memory of the electronic computer (the computations were carried out on the BÉSM-3M and M-220 electronic computers with a 4096-cell memory capacity). The computation time for one version was 2-3 min.

The total magnetic field $b = b_e + R_m b_i^*$, the electric-current densities j_x and j_y, and the magnitudes of the electrical potential and Joule dissipation currents I and I_1 were calculated from the induced magnetic fields b_i^* found as a result of solving (2.4).

The computations were performed for two unperturbed velocity profiles:

$$u_0 = 1, \quad u_0(y) = \begin{cases} \sqrt{4y} & \text{for } 0 \leqslant y \leqslant 0.25 \\ 1 & \text{for } 0.25 < y < 0.75 \\ \sqrt{4-4y} & \text{for } 0.75 \leqslant y \leqslant 1 \end{cases}$$

The functions

$$b_{e1} = \begin{cases} e^{-x^{*2}} & \text{for } x < -0.5,\ x > +0.5 \\ 1 & \text{for } -0.5 \leqslant x \leqslant +0.5 \end{cases}, \quad x^* = \begin{cases} x + 0.5 & \text{for } x < 0 \\ x - 0.5 & \text{for } x > 0 \end{cases}$$
$$b_{e2} = \frac{e^{\pi x^*/2}}{\sqrt{1 + e^{\pi x^*}}}, \qquad x^* = \frac{x}{1{,}2}$$

were considered as the applied magnetic field b_e.

The functions b_{e1} and b_{e2} and the velocity profiles $u_0 = 1$ and $u_0(y)$ are pictured schematically in Fig. 1.

To check the accuracy of the computation, the magnitude of the Joule dissipation Q calculated for the case $\beta = 0$, $R_m = 0$, $u_0 = 1$, $b_e = b_{e2}$ was compared with the value of Q obtained by the Fourier method from the solution of the Laplace equation for the potential. The comparison showed that both quantities agree to the accuracy of the first three significant figures.

Preliminary computations for applied magnetic fields b_e having breakpoints (where db_e/dx undergoes a discontinuity) showed that the quantity b_i^* is not calculated with the required accuracy in these cases. Hence, smooth functions b_{e_1} and b_{e_2} without breakpoints were selected for the analyses. The field b_{e_1} corresponds to the passage of flux through the entrance and exit zones, when the leading and trailing turns of the end currents interact; the field b_{e_2} corresponds to the case of "pure" entrance of the flux into the magnetic field.

The results of computations of the electrical characteristics of the channel are presented in Fig. 2.

Shown in Fig. 2a and b are the dependences of the total magnetic field b and the current I flowing through half the channel cross section on the coordinate x for different R_m numbers for an applied field b_{e_1}. As we see, as the magnetic Reynolds number increases, the b(x) curves shift in the direction of the motion; in turn, this results in staggering of the currents downstream in the gas. The increase in R_m is accompanied by a diminution in the magnitude of the end currents.

It is seen from Fig. 2c, d that as the Hall and magnetic Reynolds number parameters grow, the Joule dissipation diminishes; however, this diminution is insignificant for small β and R_m (~1-2).

Fig. 2e illustrates the increase in the longitudinal potential difference with the growth in the Hall parameter β [see (2.9)].

Moreover, it follows from computations of the current densities that a shift in the centers of the end-current turns from the channel axis to the wall (to the lower wall in the case under consideration) occurs in the presence of anisotropy in the conductivity. The magnitude of this shift is slight: it is 15% of the channel height for $\beta = 10$.

4. To calculate the average perturbation of the gasdynamic quantities over the cross section, the averaged electromagnetic forces and Joule dissipation found for the solution of the electrical problem were substituted into the system (1.5). The system (1.5) was then integrated by the Runge-Kutta method by a standard program. The dependences $\langle p_1 \rangle (x)$ and $\langle u_1 \rangle (x)$, calculated for the field $b_e = b_{e_1}$ in the supersonic-flow case, are presented in Fig. 3. Characteristic sections of more and less abrupt flux deceleration are noted on the curves. The sections of more abrupt deceleration correspond to flux passage through the domain of the leading and trailing turns of the end currents. As the number M_0 increases, the absolute value of the perturbations decreases. Let us note that diminution in the pressure perturbations as M_0 grows is connected with the kind of lack of measurement: $p^\circ = \rho^* v^2 p$; if the pressure refers to the unperturbed pressure $p_0^0 = p^0(-\infty)$, then the relationship $p^* = p^0/p^0(-\infty) = \gamma M_0^2 p$ will hold.

Hence, it is seen that as M_0 increases, the true pressure perturbations grow.

A calculation of the perturbation of the average gasdynamics parameters for the external magnetic field b_{e_2} showed that there is just one section of abrupt deceleration as the flux passes through the region of one turn of end current. The curves are analogous to the curves in Fig. 3 in the rest.

An increase in the Hall and magnetic Reynolds number parameters is accompanied by a diminution in the perturbations of the gasdynamics parameters averaged over the cross section, as follows from computations, and this is connected with the corresponding diminution in the Joule dissipation.

Computations performed for a subsonic flow showed that the perturbations of the mean velocity are positive in this case, while the pressure perturbations are negative.

5. Knowing the magnitudes of the electromagnetic forces and the Joule dissipation at any point of the channel, the local perturbations of the gasdynamics parameters can be found from the solution of the system (1.3). The system (1.3) was solved by the method of characteristics for the supersonic-gas-flow case.

For $M_0 > 1$ three families of characteristics exist: two families of Mach lines (first and second family characteristics) and streamlines.

The differential equations of the first and second family characteristics and their corresponding compatibility relationships are

$$dy = \pm k\,dx, \qquad k = 1/\sqrt{M_0^2 - 1}$$
$$dp_1 + (\pm k)\,dv_1 - \frac{\pm k(1 - a_0^2) f_y - a_0^2 f_x + q}{1 - a_0^2}\,dx = 0 \tag{5.1}$$

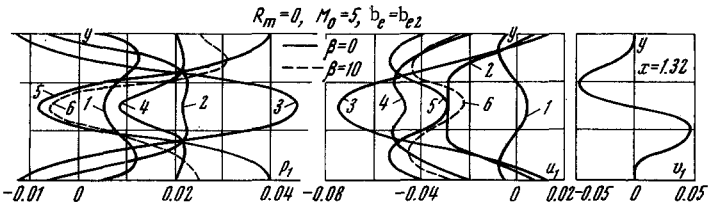

Fig. 4

Fig. 5

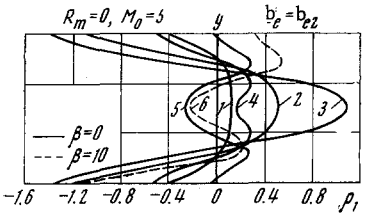

Fig. 6

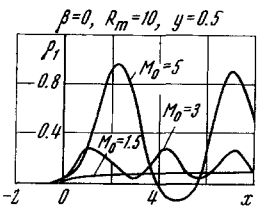

Fig. 7

The plus sign here refers to the first family characteristics, and the minus sign to the second family characteristics.

The streamlines are lines parallel to the channel axis (dy = 0). The relationships

$$du_1 + dp_1 - f_x\,dx = 0, \qquad dp_1 - a_0^2\,dp_1 - q\,dx = 0 \tag{5.2}$$

are satisfied along the streamlines.

An orthogonal mesh of points was selected for the numerical solution. The spacing h_y in the y direction was taken equal to $1/12$ for $R_m = 10$ and $1/24$ for all the remaining R_m. The spacing h_x in the x direction was determined from $h_x = h_y/2k$.

The accuracy of the computation was checked from the condition of conservation of the discharge. For $h_y = 1/12$ the difference between the discharge at the exit from the channel and the discharge given at the entrance is 2.4%, while this difference is 0.1% for $h_y = 1/24$.

The induced fields b_i^*, by means of which the electromagnetic quantities f_x, f_y, and q in (5.1) and (5.2) were determined, were calculated with an h = 0.1 spacing.

As we see, the meshes utilized to compute the electrical and gasdynamical parameters do not coincide. For convenience let us call these meshes mesh 1 and mesh 2, respectively. The values of the electromagnetic quantities at each node of mesh 2 were determined by means of known values of these quantities at the four closest nodes of mesh 1 by using linear interpolation in two directions (x and y).

Let us note that the program for a simultaneous computation of all the electrical and gasdynamical parameters with the requisite accuracy does not fit within the operational memory of the machine. Hence, to raise the accuracy of the calculations, the perturbations of the local gasdynamical parameters had to be computed by an individual program including just part of the program for the electrical problem referring to calculation of the induced fields b_i^*. The time to compute one modification was 5-6 min.

The perturbations of the local gasdynamical parameters are presented in Figs. 4-7. All the dependences presented in the graphs refer to the case of an applied magnetic field b_{e_2} (clean entrance). The solid curves appearing in Figs. 4-6 correspond to the values of the parameters $\beta = 0$, $R_m = 0$, $M_0 = 5$; while the dashed curves have been constructed for the case $\beta = 10$, $R_m = 0$, $M_0 = 5$. The numbers on the curves correspond to the following values of x:

№	1	2	3	4	5	6
$x =$	−0.317	0.5	1.32	2.85	3.56	3.44

It is seen from the figures that the gasdynamics parameters in the end current zones are distributed extremely nonuniformly over the channel section. The currents flowing in the gas exert force and thermal effects on the supersonic flux. The longitudinal electromagnetic forces in the leading half of the turn of end current act in the motion direction and accelerate the gas, while the electromagnetic forces in the

trailing half of the turn are directed oppositely to the gas motion and decelerate it. Transverse electromagnetic forces directed towards the channel axis originate at the walls; these forces are maximal in the section passing through the center of the turn. Joule-heat liberation decelerating the supersonic flux occurs within the whole volume occupied by the end current. The greatest Joule heating occurs near the walls. Let us note that the leading portion of the turn is in the domain where the magnetic field is slight. Hence, the electromagnetic forces are small here, and Joule dissipation exerts the main influence on the flux.

As a result of the mentioned effects, the pressure at the walls rises in the domain of the leading part of the run, and compression waves are propagated there from along the characteristics (Fig. 4). The pressure at the walls diminished in sections close to the center of the turn because of the transverse electromagnetic force; consequently, rarefaction domains originate at some part of the walls. Rarefaction waves are generated in these domains. The perturbations produced at the walls are propagated along the characteristics within the channel and are magnified considerably at the axis. Moreover, local perturbations which are combined with the perturbations arriving at a given point from other domains of the channel, exist at each point. Let us note that because of the inertia of the gas particles the zones of greatest perturbation of the parameters are shifted downstream relative to the zone of greatest force and thermal effects on the flux. Perturbations originating in the zone of the inhomogeneous magnetic field do not vanish after the flux has passed this zone. The propagation and reflection of the originating perturbations from the walls result in the formation of perturbations in the gasdynamical parameters which are fluctuating in structure. Analogous phenomena were noted in [11]. Under real conditions the perturbations are quenched at some distance from the end current zone because of the presence of viscosity. This examination is made in a linear approximation for an inviscid gas; hence, the perturbations are not suppressed here.

The perturbations in the longitudinal velocity (Fig. 5) are connected with the pressure perturbations. In those domains where the pressure rises, the gas is decelerated, while domains of relative acceleration of the gas (curves 4, 5) appear in the reduced pressure domains. The velocity and pressure perturbations at the walls are equal in absolute value and opposite in sign (this follows from (5.2) and the condition $f_x = 0$ at the walls). The transverse-velocity perturbations are of the same order of magnitude as the longitudinal-velocity perturbations. On the average the gas is decelerated during passage of the end current zone.

The density perturbations are shown in Fig. 6. As we see, the density perturbations for large Mach numbers M_0 are an order of magnitude greater than the velocity and pressure perturbations.

It has been mentioned in Section 3 that anisotropy in the conductivity causes a shift in the center of the end current turn to the lower wall of the channel. Consequently, the Joule dissipation and transverse electromagnetic force at the lower wall become considerably greater than at the upper wall, which results, in turn, in an essential rearrangement of the flow. The profiles of the perturbations in the gasdynamical quantities become nonsymmetric relative to the channel axis (see the dashed curves in Figs. 4, 5, 6). The density diminishes at the lower wall and increases as compared with the case $\beta = 0$ at the upper wall. Therefore, a slight asymmetry in the end current exerts a considerable influence on the distribution of the gasdynamical parameters over the channel cross section.

As computations have shown, the influence of the magnetic Reynolds number reduces mainly to a downstream shift in the current picture. The distribution of the perturbations in the gasdynamical parameters hence has the same form as for $R_m = 0$, but a noticeable perturbation in the flow is started for large values of x are compared with the case $R_m = 0$.

The Mach number of the unperturbed flux M_0 exerts a considerable influence on the perturbations of the gasdynamical parameters (Fig. 7). As has been mentioned above, the perturbations in the gasdynamical parameters are fluctuating in structure. As M_0 changes, the nature of these fluctuations changes. A growth in Mach number is accompanied by a strong increase in the density perturbations, where the velocity and pressure perturbations hence remain of the same order of magnitude as for low M_0 numbers.

In conclusion, the author is grateful to A. B. Vatazhin for useful comments and constant attention to the research and to I. U. Tolmach for valuable comments.

LITERATURE CITED

1. J. Shercliff, Theory of Electromagnetic Flow Measurements, Cambridge Univ. Press (1963).
2. A. B. Vatazhin and S. A. Regirer, Electrical Fields in Channels of MHD Apparatus [in Russian], supplement to: J. Shercliff, Theory of Electromagnetic Flow Measurements, Mir, Moscow (1965).

3. R. A. Boucher and D. B. Ames, "End effect losses in dc magnetohydrodynamic generators," J. Appl. Phys., 32, No. 5 (1961).
4. V. E. Kozyrenko, "Some new regularities in the theory of longitudinal end effects in MDH channels for arbitrary magnetic Reynolds numbers," Magnitn. Gidrodinam., 1-3, No. 1, 40-48 (1969).
5. E. A. Witalis, "Methods for the determination of currents and fields in steady two-dimensional MDH flow with tensor conductivity," J. Nucl. Energy, pt. C, 8, No. 2 (1966).
6. E. A. Witalis, "Incompressible steady flow with tensor conductivity leaving a transverse magnetic field," J. Nucl. Energy, pt. C, 8, No. 2 (1966).
7. A. E. Konovalov, "On the electrical current and potential distributions in a plane channel with point electrodes," Zh. Priklad. Mekhan. i Tekh. Fiz., No. 3 (1970).
8. A. B. Vatazhin, "Determination of the subsonic flow parameters in a channel beyond the zone of axial inhomogeneity of weak perturbing forces and heat sources," Priklad. Matem. i Mekhan., 31, No. 3 (1967).
9. L. F. Lobanova, "Problem of the entrance of a compressible gas in a homogeneous magnetic field," Zh. Priklad. Mekhan. i Tekh. Fiz., No. 6 (1964).
10. A. A. Barmin, A. G. Kulikovskii, and L. F. Lobanova, "Linearized problem of the supersonic flow at the entrance to the electrode zone of a magnetohydrodynamic channel," Priklad. Matem. i Mekhan., 29, No. 4 (1965).
11. F. D. Haynes, J. A. Joler, and E. Ellers, Hydromagnetic flux with axial symmetry in a channel, in: Ionic, Plasma, and Arc Rocket Engines [in Russian], Atomizdat, Moscow (1961).
12. W. Wasow and G. Forsythe, Finite-Difference Methods for Partial Differential Equations, Wiley (1960).
13. B. P. Demidovich and I. A. Maron, Principles of Computational Mathematics [in Russian], Fizmatgiz, Moscow (1960).